Materials Science and Engineering, 36 (1978) 231 - 239

ABO_3-Type Oxides — Their Structure and Properties — A Bird's Eye View

N. RAMADASS

Materials Science Research Centre, Indian Institute of Technology, Madras 600 036 (India)

(Received June 28, 1978)

SUMMARY

ABO_3-type oxides form an important class of materials of great technical value in several device applications. Such oxides are known to exist with a wide range of A and B ions. Most of these oxides have the relatively simple structure of the mineral perovskite ($CaTiO_3$). The ideal perovskite structure has a cubic unit cell. However, distortions are common and depend upon the value of the tolerance factor t given by $\gamma_A + \gamma_O/\sqrt{2}(\gamma_B + \gamma_O)$. Rhombohedral structure or orthorhombic $GdFeO_3$-type structure is found when t is less than unity. Polytypic structures are observed when t is greater than unity. Other structures such as ilmenite and pyrochlore also occur. ABO_3-type oxides display a wide spectrum of physical properties of technical importance such as ferroelectricity, antiferroelectricity, piezoelectricity, insulating behaviour, semiconductivity, metallic conductivity, superconductivity, ferromagnetism, antiferromagnetism etc. The ferroelectric properties are mostly controlled by the relative sizes of the ions. The electrical and magnetic properties are mainly dependent on the electronic configuration of the ions. Dopants and substituents have a profound influence on the properties of the ABO_3 oxides.

1. INTRODUCTION

Oxide materials having a composition ABO_3 form an important class since they are useful in several device applications, some examples of which follow. These materials are used in special ceramic capacitors. Piezoelectric PLZT ceramic discs made from ABO_3-type oxides are well known for their use in a variety of transducer devices such as phonograph pick-ups, strain gauges, ultrasonic equipment etc. [1]. Some doped ABO_3-type oxides find applications in switching devices [2, 3]. $LaCoO_3$ can be used instead of platinum as a catalyst in the oxidation of CO in automobile exhaust gases [4] and is also useful as an ohmic-loss-free electrode [5, 6]. $LiNbO_3$ has been used in the development of materials for generating and detecting surface acoustic waves and also in optical memory devices [7, 8]. $YAlO_3$ is a laser host material [9]. Rare earth orthoferrites are used in magnetic bubble domain devices because of their strong anisotropic properties [10].

2. STRUCTURE

Most of the ABO_3-type oxides crystallize in the relatively simple structure of the mineral perovskite ($CaTiO_3$) or in a structure closely related to it [11]. The ideal perovskite structure (Fig. 1) has a cubic unit cell of side about 3.9 Å, space group $Pm3m$ and contains one formula unit. The B ions have an octahedral oxygen coordination and the A ions have 12-fold coordination. The oxygen ions are linked to six cations (4A + 2B). If the unit cell is chosen with a B ion at the body centre, then the oxygen ions occupy the face centres and the A ions occupy the corners of the unit cell. When the A ion is assigned the body centre position, the oxygen ions are at the middle of the edges and the B ions at the corners of the unit cell. The structure can be visualized in several ways [12]. The most useful approach is to consider that it is based on that of ReO_3 with corner sharing octahedra arranged along the cube axis with the A ions occupying the interstices. The structure can also be viewed as a body-centred cubic (b.c.c.) arrangement of the A and B cations (as in CsCl) with the

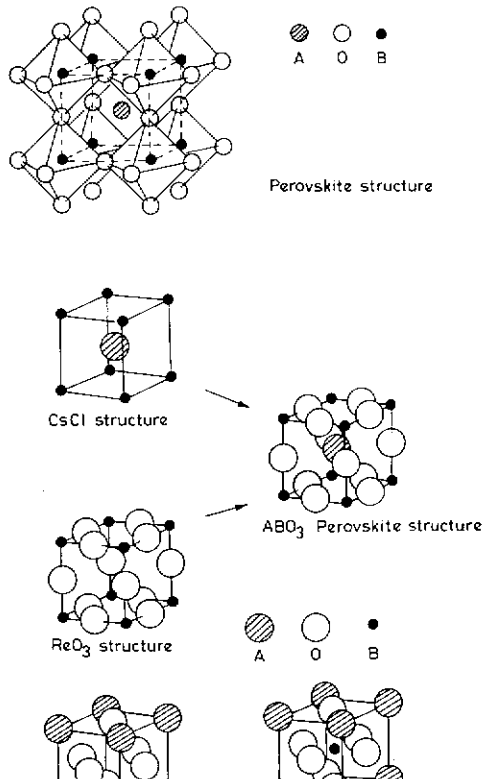

Fig. 1. Perovskite structure and its relationship to CsCl, ReO_3 and Cu_3Au structures.

oxygen ions added at the centres of the edges. It can also be considered as a face-centred close-packed AO_3 array, as in the ordered Cu_3Au structure, with the B ions occupying the octahedral hole in the centre of the unit cell.

2.1. Tolerance factor

The ideal cubic unit cell of the perovskite structure is found only in a few cases. Most of the perovskite-type oxides show distortions which give rise to important properties. Indeed, perovskite itself does not have cubic structure. The essential requirement for the stability of the perovskite structure is that the A and B ions should be of a suitable size to form 12-fold and 6-fold (octahedral) anion coordination respectively ($\gamma_A > 0.9$ Å and $\gamma_B > 0.51$ Å). If we assume that the ions are in contact with each other, it can be seen from the geometry of the unit cell that $(\gamma_A + \gamma_O) = \sqrt{2}(\gamma_B + \gamma_O)$ in the ideal case. However, the perovskite structure is formed even if this relation is not followed exactly. Goldshmidt [13] has defined the tolerable variation limits for the radii γ_A and γ_B by the tolerance factor $t = (\gamma_A + \gamma_O)/\sqrt{2}(\gamma_B + \gamma_O)$. Perovskite-type structure is usually obtained in the range $0.75 \leqslant t \leqslant 1.0$. For the ideal perovskite structure $t = 1$. The limiting values of t may differ depending upon the set of ionic radii employed. The set of ionic radii proposed by Shannon and Prewitt [14] is commonly employed in crystal chemical considerations. In a particular group of ABO_3 oxides the approach to ideal structure can be predicted as t approaches the ideal value of unity by using a self-consistent set of ionic radii. Empirical modifications have been made on this factor to take account of the relative strengths of the A—O and B—O bonds [15].

2.2. Deviations from perovskite structure

2.2.1. t < 1

As t decreases from 1, the perovskite structure deforms towards structures with lower coordination for A. When it is slightly less than unity a rhombohedral distortion usually results. Although the normal X-ray patterns in these cases can be indexed on a perovskite-type pseudo-cell with rhombohedral angle $\alpha \approx 90°$, faint lines observed in careful X-ray studies [16] have indicated that at room temperature the anionic displacements demand a doubling of the c axis. Usually a larger unit cell containing two formula units is chosen with $\alpha \sim 60°$ and $a \sim \sqrt{2}\ a_o$ (where a_o is perovskite-type pseudo-cubic cell dimensions). A face-centred rhombohedral cell with four formula units and $a \approx 2a_o$ or a triply primitive hexagonal unit cell are also possible. The symmetry may be $R\bar{3}c$, $R\bar{3}m$ or $R\bar{3}$ depending on the nature of displacements of ions from ideal cubic perovskite and is difficult to distinguish by X-ray structure studies alone. The distortion to $R\bar{3}c$ occurs by a cooperative rotation of the BO_6 octahedra along the ⟨111⟩ direction with the AO_3 layers remaining equidistant from the B ion (111) layers. This results in a decrease in three A—O bond lengths and an increase in the other three A—O bond lengths. The $R\bar{3}m$ symmetry results from the creation of two kinds of B sites. At one of these sites the octahedron contracts by movement of O^{2-} ions (along the B—B axis) closer to the central B ion. At the other site the octahedron expands by movement of O^{2-} ions away from the centre. $R\bar{3}$

symmetry is found when both types of displacement ($R\bar{3}c$ and $R\bar{3}m$) occur simultaneously. In the doubly primitive rhombohedral unit cell the A ions are at the position $2a$: $\pm(0.0,1/4)$, the B ions at $2b$: (0,0,0; 0,0,1/2) and the oxygen ions are at $6e$: $\pm(x,0,1/4$; $0,x,1/4$; $\bar{x},\bar{x},1/4$) [17]. The greater the deviation of the oxygen parameter x from the ideal value of 1/2, the greater is the distortion of the coordination polyhedron around A resulting in 8-fold coordination in $GdFeO_3$ type structure.

2.2.2. t close to the lower limit of 0.75

When t is near the lower limit for perovskite-type structure formation, the distortions lead to a larger orthorhombic unit cell. A large number of these orthorhombic perovskites, especially those featuring trivalent A and B ions [18 - 22], have a structure typified by that of $GdFeO_3$ which may also be regarded as a new structure type. The orthorhombic unit cell has the space group *Pnbm* identified readily by the absence of $(h0l)$ reflections with $(h + l)$ odd and $(0kl)$ reflections with k odd in the X-ray diffraction pattern. There are four formula units in the unit cell. The A cations are in position 4c, the B ions in 4b, the O_I^{2-} ions in 4c and the O_{II}^{2-} ions in 8d. The cell parameters a and b are about $\sqrt{2}a_o$ and $c \approx 2a_o$ where a_o is the side of the pseudocubic perovskite cell. The orthorhombic dimensions a and b are along the cubic ⟨110⟩ and ⟨1$\bar{1}$0⟩ directions and c is along the ⟨001⟩ direction. The perovskite-type pseudo-cell with one formula unit is monoclinic for this structure. Projections of two perovskite-type quarters of the orthorhombic unit cell on the (001) plane are shown in Fig. 2. In simple perovskites these parts would be cubes and would project on as a square with A ions at the corners, O^{2-} ions at the middle of the edges and B ions in the centre. The essential difference between the ideal perovskite and $GdFeO_3$ structures is in the coordination around the A ion and the orientation of the BO_6 octahedra. In $GdFeO_3$ the chains of octahedra are buckled to optimize the A—O bond lengths. The B–O–B angle ranges from 140° to 155°. In the ideal perovskite it is 180°. The AO_{12} polyhedron is severely distorted with O–A–O angles deviating from 90°. The twelve A—O bond lengths which are equal in cubic perovskite

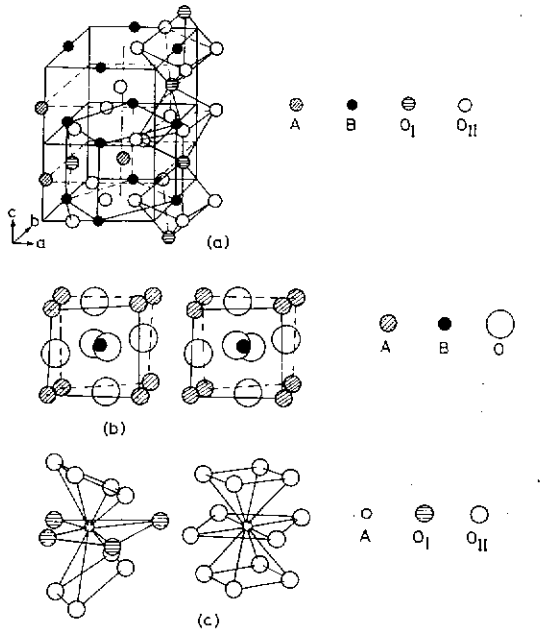

Fig. 2. (a) Structure of $GdFeO_3$; (b) projections of perovskite-like pseudo cells of $GdFeO_3$ structures on to the (001) plane; (c) AO_{12} polyhedron in $GdFeO_3$ structure and ideal perovskite structure.

show a large variation [21]. The A—O bond lengths in the typical case of $GdFeO_3$ are $4O_I^{2-}$ at 2.26, 2.36, 3.19 and 3.41 Å and $8O_{II}^{2-}$ at 2.38 (2), 2.39 (2), 2.82 (2) and 3.48 (2) Å. From this it can be seen that the A ions are essentially 8-coordinated with the remaining $4O^{2-}$ ions at a greater distance. The environment of the A ion is shown in Fig. 2. However, the B ions retain their octahedral coordination in the $GdFeO_3$ structure. The Fe—O bond lengths are 2.01 (2), 2.08 (2) and 1.95 (2) Å. In some cases (*e.g.* $LaFeO_3$) the positions of A and O^{2-} show a deviation from ideal perovskite [22] although the cell dimensions may be close to cubic ($a = b = c/\sqrt{2}$).

The adoption of the $GdFeO_3$ structures for many ABO_3 oxides appears to be determined mainly by size effects. Other considerations such as magnetic interactions, electronic configuration of the ions etc. play only a secondary role. This is indicated by the fact that several rare earth scandates, vanadates, chromates, manganates, ferrites, cobaltates, gallates and aluminates featuring a variety of B ions occur in this structure. It is evident that it is the size effect that controls the distortion of the perovskite structure in this series of oxides if one considers the fact that for a given B ion the distortion decreases as

the radius of the A ion increases (t increases). Thus in $LnFeO_3$ ferrites, $YFeO_3$ which has the small Y^{3+} as the A ion shows the largest deviation [21]. The atomic positions and cell dimensions approach the ideal cubic as we pass from the smaller rare earths to lanthanum, with $LaFeO_3$ having nearly cubic cell dimensions. The $GdFeO_3$ structure is linked to the ideal perovskite by the rhombohedral structure. For example in aluminates, the orthorhombic structure is found for smaller rare earth ions, whereas for lanthanum, neodymium and praseodymium the rhombohedral structure is found. The samarium ion is a border line case since it shows a transition to the rhombohedral structure upon heating. The rhombohedral perovskites transform to cubic structure at higher temperatures (*e.g.* $LaAlO_3$). The transformation from the orthorhombic to the rhombohedral form occurs by converting the twelve oxygens around A into two equivalent sets of six taking four from the 8d sites and two from the 4c sites.

2.2.3. When $t \approx 1$

When t is close to or slightly greater than unity, spontaneous ferroelectric distortions of the cubic unit cell to lower symmetry occur by slight displacements of the B ion within the octahedra, as in $BaTiO_3$. However, there are no large structural deviations in these ferroelectric phases.

2.2.4. When $t > 1$

When the A ion is very large ($t > 1$) the distortions of the perovskite structure lead to closely related polytypic phases in which some of the octahedra share faces instead of corners [23 - 30]. In the ideal perovskite structure, BO_6 octahedra share only corners forming a three-dimensional network. The A ions occupy the cubic voids formed by the B–O–B links. The size of the A ion that can be accomodated in this void is limited by the characteristic length of the B—O bond which determines the size of the void. If the size of the A ion is increased beyond this limit, the B–O–B links are strained and the octahedra are forced to share faces. In the extreme case all the octahedra share only faces as in $BaNiO_3$ [23] (Fig. 3). The face-linked octahedra form infinite strings running parallel to the c axis. Since the strings are not interlinked, the bigger A ion is accommodated by adjustment of spacing between the strings. The transformation from all cubic (ideal perovskite) to all face-sharing ($BaNiO_3$) occurs through the formation of polytypic structures where both the characteristics are found. The polytypes are defined as different structural modifications of a given composition, having similar unit cells in two dimensions but different stacking of layers along the third axis to make its variable length an integral multiple of some common unit.

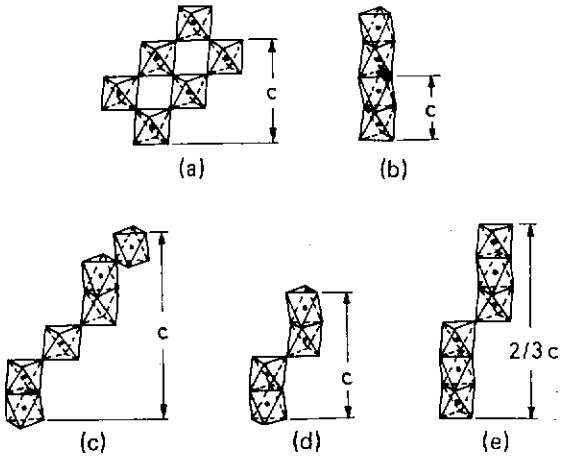

Fig. 3. Arrangement of octahedra in the (110) plane of the hexagonal cell in some polytypic strucutres: (a) $BaTiO_3$ (cubic, 3C); (b) $BaNiO_3$ (hexagonal, 2H); (c) $BaTiO_3$ (hexagonal, 6H); (d) $BaMnO_3$ (hexagonal, 4H); (e) $BaRuO_3$ (hexagonal, 9H).

Since in these cases the size of the A ion is comparable with that of the oxygen ion, the relation between the different polytypes could be rationalized on the basis of stacking of close-packed AO_3 layers. The different polytypes are generated by periodic variations in the stacking sequence along the c axis from cubic to hexagonal. In the hexagonally stacked layers the octahedra share faces and in the cubic layers they share corners. An infinite number of stacking sequences are possible in principle. However, only a few combinations have been found so far. The structures are denoted by the number of AO_3 layers present along the c axis of the unit cell. Thus 6H implies six layers in the c axis and a hexagonal unit cell. Structures having up to 27 layers are reported [28].

That it is the relatively large size of the A ion which leads to the formation of polytypes is shown by the fact that for a given B ion the face-sharing in polytypes decreases progres-

sively as the size of the A ion is decreased (t decreases) leading ultimately to the simple perovskite structure. Similarly, for a given A ion the face sharing progressively decreases as the size of the B ion is increased. The presence of d electrons in B ions favours face sharing by the formation of metal–metal bonding. The short B—B distances in the polytypes indicate the occurrence of this kind of bonding. That d electrons favour face sharing is also exemplified by the fact that $BaTiO_3$, which adopts the corner-shared perovskite structure, can normally be obtained in the hexagonal polytype form when slightly reduced since reduction creats Ti^{3+} ions (Ti^{4+}:d^0, Ti^{3+}:d^1).

2.3. Structures not related to perovskite

The majority of ABO_3-type oxides adopt one of the perovskite-related structures. A relatively small minority of ABO_3 type oxides occur in structures not related to perovskite.

2.3.1. Defect pyrochlore-type structure

Pyrochlore is denoted by the composition $A_2B_2O_7$. It has a cubic unit cell of dimensions about 10.5 Å with space group $Fd3m$. The structure consists of a skeleton of composition B_2O_6 formed by BO_6 octahedra sharing corners (B ions in 16d sites and O ions in 48f sites). The seventh oxygen (8a sites) and the A ions (16c sites) occupy the open cages in the network. The A ions have a nearly hexagonal bipyramidal coordination of oxygen atoms. The 48f oxygen atoms have a tetrahedral coordination of 2A and 2B ions. The seventh oxygen (8a) atom has a tetrahedral coordination of four A ions [31]. This oxygen is only loosely bound to the structure and can be removed progressively ultimately giving the composition $A_2B_2O_6$ (equivalent to ABO_3). ABO_3 oxides having A ions like Tl^+, Pb^{2+} and Bi^{3+} prefer to occur in this defective pyrochlore structure. For example $PbRuO_3$, $PbReO_3$, $TlNbO_3$, $TlTaO_3$, $BiRhO_3$ etc. have been found to adopt this structure [32 - 34]. The removal of 8a anions to form the defect pyrochlore structure exposes the A cations to each other across the 8a vacancy. The stability of the defect pyrochlore structure has been explained in terms of bonding between the A cations through this oxygen vacancy [32]. This has been called a "trap-mediated" bond. In effect this implies a polarization of A cations by the virtual positive charge of the oxygen vacancy resulting in a stabilization of the $6s^2$ polarizable electrons. Electron density maps from X-ray diffraction also indicate a significant electron density at the vacancy sites [32]. These defect pyrochlores transform to perovskites at high pressures.

2.4.2. Ilmenite-type structure

Among the non-perovskite-type structures for the ABO_3 oxides, the ilmenite structure is most frequent. This structure is taken up if the size of the A ion is very small and comparable with that of the B ion as in $FeTiO_3$, $NiTiO_3$ etc. Here t is lower than the limit for perovskite. Borderline cases are possible. For example, the ilmenite type $CdTiO_3$ transforms to perovskite at higher temperatures [12]. The ilmenite structure is essentially the same as that of corundum (Al_2O_3) and consists of hexagonally stacked oxygen layers along the c axis. The cations occupy two-thirds of the octahedral holes (between the layers) in an orderly fashion such that planes of A and B ions occur alternately along the c axis [12].

3. PROPERTIES

ABO_3 oxides display a wide spectrum of special physical properties such as ferroelectricity, piezoelectricity, semiconductivity, metallic conductivity, superconductivity, paramagnetism, ferromagnetism etc. These properties are controlled by several parameters such as ion size, electronic configuration and preparative conditions.

3.1. Ferroelectricity and associated properties

Ferroelectricity was first discovered in oxide materials in the ABO_3-type oxide $BaTiO_3$. This led to a search for new ABO_3 oxides of this type and a study of their characteristics. Ferroelectricity in ABO_3 oxides is mainly controlled by the sizes of the A and B ions. It is generally found in perovskite-type oxides with small B ions like Ti^{4+}, Nb^{5+}, Ta^{5+} etc. and large A ions like K^+, Ba^{2+}, Pb^{2+} etc. The size of the octahedral interstice formed by AO_3 layers with large A ions like Ba^{2+} is also large, with the result that the small B ions

can rattle in the octahedral hole. Hence at low temperatures the B ions are slightly displaced from the centre of symmetry of the BO_6 octahedron. This in effect implies the creation of a dipole. Spontaneous polarization of the structure occurs when these displacements are cooperative, with all the dipoles oriented in one direction. For the tetragonal form of $BaTiO_3$ the direction of displacement is ⟨001⟩. Application of an electric field along this axis pushes the Ti^{4+} ions to the equivalent position in the opposite side of the centre of symmetry. Thus the dipole orientation can be reversed by external fields, which gives rise to hysteresis and ferroelectricity. In the orthorhombic form the displacement is along the ⟨110⟩ direction and in the rhombohedral form it is along the ⟨111⟩ direction [35, 36]. The symmetry increases progressively with increasing temperature in the order rhombohedral → tetragonal → cubic, owing to an increase of vibration of Ti^{4+} within the octahedral hole. Since there are no static displacements of Ti^{4+} in the high temperature cubic form, no spontaneous polarization is observed. The temperature of transition to the non-ferroelectric form is called the Curie temperature. The effect of the size of the ions is clearly shown by the fact that when Sr^{2+}, which has a smaller size than Ba^{2+}, is substituted for the Ba ion the Curie temperature is lowered [37]. This is because the size of the octahedral hole is reduced and hence the tendency for the B ion to vibrate is also lowered. Similarly if Zr^{4+}, which has a larger size than Ti^{4+}, is substituted for the Ti ion in $BaTiO_3$ the Curie temperature decreases [38].

In some ABO_3 oxides like $PbZrO_3$ the displacements of the B ions in adjacent unit cells occur in such a way that no residual dipole occurs. Compounds which have opposing alignment of dipoles are called antiferroelectrics. In this case it is also possible to orient all the dipoles in the same direction by the application of strong fields [39].

The unit cell of ferroelectric perovskites lacks a centre of symmetry and therefore they are also piezoelectric. Many applications of the ABO_3-type oxides as transducer materials are based on the piezoelectric behaviour. These are used to convert electrical pulses into mechanical oscillations and vice versa. The great advantage of perovskite ceramics over conventional piezoelectrics like quartz is that they have both ferroelectric and piezoelectric properties. Their ferroelectric nature is utilized to orient the axis of maximum piezoelectric activity, even in ceramic bodies of complicated shape, by poling them in the desired direction. This is not possible in other piezoelectrics. Other properties of the ferroelectric perovskites such as square hysteresis loops, high dielectric constant, non-linear polarization, high remanent polarization and electrooptic effects have also been put to use [35].

3.2. Magnetic and electrical properties

These properties are mainly controlled by the electronic configuration of the ions [40 - 43]. Interesting characteristics arise from the d electrons of transition metal ions at the B site.

A variety of types of magnetic behaviour has been encountered. Ferromagnetism in perovskites was first found by Jonker and Van Santen [44] in the $LaMnO_3$ system. Antiferromagnetism or weak ferrimagnetism is found in several rare earth ferrites. Pauli paramagnetism is found in $SrVO_3$ and $LaNiO_3$. Simultaneous ferroelectric and ferromagnetic behaviour has been found in the $LaMnO_3$–$BaTiO_3$ system [45]. Simple Curie–Weiss behaviour has been found in many cases. In perovskites the magnetic interaction between the A ions is very weak compared with that between the B ions. However, the direct interaction between B ions is negligible owing to the large distance between them in contrast to that in rocksalt-type oxides like NiO. The coupling between the spins of adjacent B ions occurs mainly by a 180° superexchange interaction involving the oxygen ions which link the B ions. The nature and magnitude of this interaction depend on the electronic configuration of the B ion [11]. When both the interacting B ions are of type $t_{2g}^{x}e_g^{2}$ (t_{2g}^{x}, partially filled t_{2g} orbitals) or $t_{2g}^{3}e_g^{0}$ the interaction is antiferromagnetic. Ferromagnetic interaction occurs in cases where one of the B ions is of type $t_{2g}^{6}e_g^{2}$ and the other is $t_{2g}^{3}e_g^{0}$ or where one is of type $t_{2g}^{x}e_g^{2}$ and the other is $t_{2g}^{3}e_g^{0}$. Ferromagnetism can also result from a double exchange phenomenon [11] when there is a non-integral number of d electrons per B cation (due to non-stoichiometry) as in $LaMnO_3$. In such cases electron spin is con-

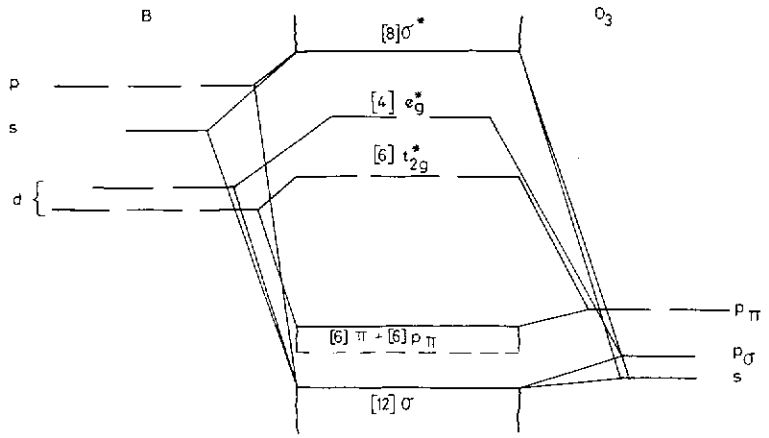

Fig. 4. Electronic energy level scheme for perovskite structure.

served during the movement of the charge carriers by electron transfer. This causes a coupling of the spins of neighbouring atoms parallel to one another.

The electrical properties of the ABO_3 oxides vary widely. Oxides like $BaZrO_3$ exhibit insulating behaviour since there are no d electrons at the B site atoms. Some oxides like $LaFeO_3$ have high resistivity although the B ion has d electrons. Metallic conduction and Pauli paramagnetism are observed in some of them such as $SrVO_3$ and $SrRuO_3$. Most of the ABO_3 oxides are semiconductors.

The electronic energy level diagram for perovskite-type ABO_3 oxides is given in Fig. 4. The scheme has been arrived at by considering mainly the covalent interaction between B and O^{2-} ions [11]. The electrical properties are primarily dependent on the B–O interaction. When the overlap between the orbitals of B and O^{2-} is small, the orbitals are localized and semiconducting behaviour is observed. When the overlap integral is greater than a critical value Δ_c the orbitals become collective. If the collective orbitals are only partially filled metallic conductivity results. When the π bonding between B and O^{2-} is large ($\Delta^{\pi}_{cac} > \Delta_c$), the $t_{2g}{}^x$ orbitals become a collective π^* band. This is probably the case in metallic $LaTiO_3(d^1)$. When σ bonding is large the $e_g{}^*$ levels become a collective σ^* band as in $LaCoO_3$ at high temperature [43].

The A–O interaction modifies the effect of the B–O interaction in controlling the electrical properties. This is clearly revealed by the trends of the electrical conductivity in the series of rare earth vanadates $LnVO_3$ [46 - 49]. $LaVO_3$ has a high electrical conductivity (nearly metallic). However, as we pass from lanthanum to the other rare earths, the electrical conductivity progressively decreases and the activation energy for conduction increases. This is due to the increase in acidity of the Ln^{3+} ions as we pass from La^{3+} to the smaller rare earths. This increased acidity increases the A–O interaction which tends to decrease the effect of B–O interactions. Hence the metallic nature decreases.

3.3. Effect of substituents on electrical properties

Partial substitution for A or B ions may also influence the electrical properties significantly. For example in $LaCoO_3$ progressive substitution by strontium for lanthanum gradually imparts a metallic character [50]. This is due to the creation of Co(IV) ions at the B site for charge compensation. Because of its higher charge Co(IV) enhances the covalent nature of the B–O interactions and hence enhances the metallic nature. $LaRuO_3$ is metallic. A 10% substitution by Fe^{3+} for Ru^{3+} destroys the metallic nature of $LaRuO_3$ completely [51]. In some cases, such as the ferroelectric $BaTiO_3$, even less than 0.5% substitution of lanthanum for barium can lower the electrical resistivity enormously (by three to five orders of magnitude [52]) owing to the introduction of charge carriers into the conduction band by doping. Such ABO_3 oxides sometimes show an anomalously high positive temperature coefficient of resistance (PTCR) at the ferroelectric Curie point (120 °C). However, the PTCR is con-

trolled more by preparative conditions such as grain size, formation temperature, oxygen partial pressure etc. than by the electronic configuration of the ions [53]. Similarly in the metallic oxide $BaPbO_3$, a 5 - 30% substitution of bismuth for lead induces superconductivity [54]. However, the exact mode of action of the substituent is not clearly established in this case. Generally ABO_3 oxides are electronic conductors. Ionic conduction is not favoured because of the close-packed nature of the perovskite structure. However, it has recently been found that substitution in some ABO_3 oxides can lead to ionic conduction. Thus partial substitution by aluminium in $CaTiO_3$ gives rise to ionic conductivity close to that observed in oxides with the fluorite structure [55]. Substitution by lower valence ions of fixed valency at the B site in these ABO_3 oxides creates oxygen vacancies for charge neutrality. This increase in the oxygen ion mobility and oxygen ionic conduction is observed.

ACKNOWLEDGMENTS

The author is thankful to the CSIR, India, for financial support. Assistance by Dr. G. Nagasubramanian, Mr. K. Chandrasekaran, Mr. M. A. Subramanian and Mr. K. C. Venkatanarayanan is gratefully acknowledged.

REFERENCES

1 B. Jaffe, W. R. Cook and H. Jaffe, Piezoelectric Ceramics, Academic Press, New York, 1972.
2 H. Braver and E. Fenner, Siemens Rev., 3 (1965) 95.
3 H. Kaiser, Siemens Rev., 40 (1973) 475.
4 R. J. H. Vorehoeve, J. P. Remeika, P. E. Freeland and B. T. Mathias, Science, 177 (1972) 353.
5 C. S. Tedmon, Jr., H. S. Spacil and S. P. Mitoff, J. Electrochem. Soc., 116 (1969) 1170.
6 D. B. Meadowcroft, Nature (London), 226 (1970) 847.
7 F. S. Hickernell, J. Solid State Chem., 11 (1975) 225.
8 D. L. Staebler, J. Solid State Chem., 12 (1975) 177.
9 B. Cockayne, in B. Cockayne and D. W. Jones (eds.), Modern Oxide Materials, Academic Press, New York, 1972.
10 R. C. Sherwood, J. P. Remeika and H. J. Williams, J. Appl. Phys., 30 (1959) 217.
11 J. P. Goodenough and J. M. Longo, Landolt-Bornstein Tabellen, New Series, III/4a, Springer Verlag, Berlin, 1970.
12 F. Galasso, Structure and Properties of Inorganic Solids, Pergamon, New York, 1970.
13 V. M. Goldshmidt, Skr. Nor. Vidensk. Akad. Oslo, 2 (1926).
14 R. D. Shannon and C. T. Prewitt, Acta Crystallogr., Sect. B, 25 (1965) 925.
15 O. Fukunga and T. Fujita, J. Solid State Chem., 8 (1973) 331.
16 S. Geller, Acta Crystallogr., 10 (1957) 243.
17 B. Derighetti, J. E. Drumhller, F. Laves, K. A. Muller and F. Waldner, Acta Crystallogr., 18 (1965) 557.
18 S. Geller, J. Chem. Phys., 24 (1956) 1236.
19 S. Geller and E. A. Wood, Acta Crystallogr., 9 (1956) 563.
20 S. Geller and V. B. Bala, Acta Crystallogr., 9 (1956) 1019.
21 P. Coppens and M. Eibschutz, Acta Crystallogr., 19 (1965) 54.
22 M. A. Gilleo, Acta Crystallogr., 10 (1957) 161.
23 J. J. Lander, Acta Crystallogr., 4 (1951) 148.
24 L. Katz and R. Ward, Inorg. Chem., 3 (1964) 205.
25 P. C. Donohue, L. Katz and R. Ward, Inorg. Chem., 4 (1965) 306.
26 P. C. Donohue, L. Katz and R. Ward, Inorg. Chem., 5 (1966) 335.
27 J. M. Longo and J. A. Kafalas, Mater. Res. Bull., 3 (1968) 687.
28 B. L. Chamberland, Inorg. Chem., 8 (1969) 286.
29 T. Negas and R. Roth, J. Solid State Chem., 3 (1971) 323.
30 B. L. Chamberland, A. W. Sleight and J. F. Weiher, J. Solid State Chem., 1 (1970) 506.
31 F. Jona, G. Shirane and R. Pepinsky, Phys. Rev., 98 (1955) 903.
32 J. M. Longo, P. M. Raccah and J. B. Goodenough, Mater. Res. Bull., 4 (1969) 191.
33 J. M. Longo, P. M. Raccah, J. A. Kafalas and J. W. Pierce, Mater. Res. Bull., 7 (1972) 137.
34 N. Ramadass, T. Palanisamy, J. Gopalakrishnan, G. Aravamudan and M. V. C. Sastri, Solid State Commun., 17 (1975) 645.
35 J. C. Burfoot, Ferroelectrics, Van Nostrand, London, 1967.
36 H. D. Megaw, Ferroelectricity. In Crystals, Methuen, London, 1967.
37 G. Shirane and A. Takeda, J. Phys. Soc. Jpn., 6 (1951) 128.
38 T. N. Verbitskaya, G. S. Zhadnov, Yu. N. Venevtsov and S. P. Solvev, Kristallografiya, 3 (1958) 186.
39 M. Wolters, C. L. H. Thieme and A. J. Burgraf, Mater. Res. Bull., 11 (1976) 315.
40 J. B. Goodenough, J. Appl. Phys., 37 (1966) 1415.
41 J. B. Goodenough, Czech. J. Phys., B17 (1967) 304.
42 J. B. Goodenough, J. Appl. Phys., 39 (1968) 403.
43 P. M. Raccah and J. B. Goodenough, Phys. Rev., 155 (3) (1967) 932.

44 G. H. Jonker and J. H. Van Santen, Physica, 16 (1950) 337.
45 Yu. Ya. Tomashpolskii and Yu. N. Venevtsev, Kristallographfiya, 11 (1966) 731.
46 B. Reuter and M. Wollnick, Naturwissenschaften, 17 (1963) 569.
47 P. Dougier and A. Cassalot, J. Solid State Chem., 2 (1976) 396.
48 T. Palanisamy, J. Gopalakrishnan and M. V. C. Sastri, Z. Anorg. Allg. Chem., 415 (1975) 275.
49 T. Sakai, G. Adachi and J. Schiokawa, Mater. Res. Bull., 11 (1976) 1295.
50 P. M. Raccah and J. B. Goodenough, J. Appl. Phys., 30 (1968) 1209.
51 R. J. Bouchard, J. F. Weiher and J. L. Gillson, J. Solid State Chem., 21 (1977) 135.
52 G. H. Jonker, Solid State Electron., 7 (1964) 895.
53 H. Ueoka and M. Yodogawa, IEEE Trans. Manuf. Technol., 3 (1974) 77.
54 A. W. Sleight, J. L. Gillson and P. E. Bierstadt, Solid State Commun., 17 (1975) 27.
55 K. W. Browall, O. Muller and R. H. Doreonous, Mater. Res. Bull., 11 (1976) 1475.